AIAA Paper 93-3080, 24th Fluid Dynamics Conference, July 1993

SCV MEASUREMENTS IN THE WAKE OF A ROTOR IN HOVER AND FORWARD FLIGHT

R.B. Funk§, P.A. Fawcett†, N.M. Komerath‡
School of Aerospace Engineering
Georgia Institute of Technology
Atlanta, Georgia 30332-0150

ABSTRACT

Progress in the capability to measure instantaneous velocity fields in complex flows and over large areas is discussed. The rotor wake is a complex flow field containing a wide range of velocity scales that exhibit a periodic variation with rotor azimuth. The measurement of instantaneous planar velocity fields over large areas in such flows is demonstrated using Spatial Correlation Velocimetry. A dual video camera system is used to obtain images over short intervals, with velocities computed using a fully numerical procedure. Results are presented for twelve azimuth positions in the wake of a 2-bladed teetering rotor of 0.457m radius, at 1050 rpm in low-speed forward flight, with smoke in the flow illuminated using a pulsed laser sheet. Detection of a roll-up under the rotor hub is discussed. A second area of application is shown in the measurement of turbulence statistics in recirculating flows over large areas. The recirculating flow in a 4.88 m rotor hover test facility is measured piecewise. Ensemble-averaging of local mean and root-mean-square velocity components is presented, with incoherent light sheets created from quartz lamps. Problems encountered and possible solutions are also discussed.

INTRODUCTION

Over the past three years, the technique of Spatial Correlation Velocimetry (SCV) has advanced from very slow flows in water channels (Ref. 1) to instantaneous velocity fields in fully unsteady and turbulent air flows around complex configurations. In this paper we describe recent advances in two areas where the technique shows unique capabilities. The first is the measurement of instantaneous velocity fields in the wake of a rotor in forward flight in a 2.1 x 2.5 m wind tunnel. Here the challenge is to capture and analyze a sufficient number of velocity fields to resolve the periodic variation of the velocity field. This experiment also involves a wide range of spatial and temporal scales of velocity variation, as well as a highly three-dimensional flow field with strong out-of-plane velocities. The second application is the measurement of velocity statistics over large areas, using ordinary white light sources. This opens the door to full-scale planar velocity measurement in a variety of applications.

BACKGROUND

Unlike the various techniques collectively known as Particle Image Velocimetry, there is no need in SCV to resolve individual particles. The basic premise is that most of the energy of the flow is contained in larger "packets" of fluid. Even in highly turbulent flows the size of these "packets" is much larger than the size of the individual particles. These "packets," imaged twice with a sufficiently small time delay, remain largely undistorted, exhibiting a spatial displacement that can be determined computationally. The freedom from the need to image individual particles allows the technique to be applied to large areas. Since no properties of coherent light are essential to the technique, laser sources can be replaced by inexpensive white-light sources which can be scaled up. Since the post-processing is entirely computational, a variety of iterative algorithms can be used, and the speed of the technique is limited only by computational speed.

PREVIOUS WORK

SCV has been demonstrated previously on both steady and unsteady configurations. Ref. 1 outlines the theoretical basis. Ref. 2 describes the technique applied to low speed flow over a wing at a steady, small angle of attack and then to the same wing executing large-amplitude plunging motion, with intermittent flow reversal. Most recently presented were results of a canard wing experiment in Ref. 3. This experiment demonstrated the applicability of SCV to large area and higher speeds and the analysis of a continuously changing configuration.

---

§ Graduate Research Assistant. Student Member, AIAA.

† Former Graduate Research Assistant. Member, AIAA.

‡ Associate Professor. Senior Member, AIAA.

The canard wing experiment was conducted in the John J. Harper 2.1m x 2.5m Wind Tunnel at Georgia Tech. The wing was a UH-1 helicopter stabilator with a span of 1.194m and a chord of 0.813m, the canard had a NACA 0012 section with a span of 1.067m and a chord of 0.234m. The tunnel was run at 6.1 m/s. While the aspect ratio of the wing was too small for basic studies of canard wing interactions, the experiment served to demonstrate SCV over large areas at higher speeds. Eighteen image pairs were captured and analyzed from a 2 minute and 7 second portion of video tape. During this segment, the canard changed angle of attack and translated both vertically and horizontally. Fig. 1 is an example of the vector plots from the analysis of the experiment. This vector plot shows the perturbation of the stalled canard on the wing as the canard moves vertically downward. This experiment demonstrated extraction of quantitative, instantaneous planar velocity data from flow-visualization experiments over large areas. It also demonstrated the ability to study quasi-steady flows where a configuration is being continuously varied in a single experiment.

PRESENT EXPERIMENTS

The current experimental imaging set-up is shown in Fig. 2. Two intensified video cameras are externally synchronized so that the shutter of one camera has a small time delay relative to the other. The length of this time delay is determined by the area and the velocities being studied. The cameras are aligned to focus on the same area of a flow field illuminated by a light sheet seeded with smoke or atomized liquid particles introduced into the flow. The visualization is then recorded on two VCRs, and frame-coded. Corresponding images from the two cameras are captured using frame grabber hardware in an Intel 80486 based microcomputer. The spatial cross correlation is either performed on the same platform or the images are transferred and analyzed on a CM-2 Connection Machine, a massively parallel supercomputer at the Pittsburgh Supercomputer Center.

Current work aims to apply the SCV technique to more complicated flow fields such as those encountered in a rotor wake. The rotor wake contains concentrated vortices with large velocity gradients and also is a highly three dimensional flow field. These factors present challenges to the application of SCV. An additional area of exploration is the application of SCV to large areas. This capability is useful for obtaining course velocity fields around full scale test articles and also for study of velocity fields in the wakes of ships or buildings where rotorcraft would be operating. Experiments with SCV in both of these areas are presented in this paper.

ROTOR WAKE EXPERIMENTS

Experimental Setup

For these experiments the John J. Harper 2.1 x 2.5 m wind tunnel was configured as a forward flight rotor test facility. A rotor shaft mounted through the ceiling of the test section was used to drive a 0.914 m diameter fixed pitch rotor. The rotor advance ratio was varied by changing the rotor RPM or the freestream speed. For the first set of measurements, a wing of chord 0.813 m and low aspect ratio was present below the rotor as shown. During the second experiment the wing was removed. The two camera system previously described was used in this experiment focusing on areas beneath the rotor. The camera shutters were set at 1/8000 sec. A pulsed copper vapor laser was used to create a light sheet below the rotor and parallel to the free stream. The flow was seeded with a smoke wire located upstream. A third camera was mounted above the test section focused on an azimuth disk fixed to the rotor shaft. This image was inserted into the flow visualization to provide a record of rotor position at each frame and allowed sorting of the frames by azimuth during post-processing. A schematic of the setup is shown in Fig. 3 showing the areas studied. The experiments were run at a rotor advance ratio of 0.075: 1050 RPM rotor speed, 4.6 m/s tunnel freestream speed.

Results

Rotor hub flow

For the first experiment with the wing below the rotor, image pairs were obtained at 30 degree intervals of rotor azimuth, resulting in twelve velocity plots for a full rotor rotation. The area under the rotor covered by each image was 22.4 x 16.8 cm. A total of 60 image pairs were acquired and analyzed, five for each azimuth location. Periodicity of the rotor wake was assumed and these results were then averaged at each azimuth location. The results are shown in Fig. 4. The results are presented in terms of pixel shifts due to uncertainty in determination of the time delay between the images. This was in part due to the pulsing of the laser not being synchronized with the camera triggering pulses. Triggering of the laser using an external pulse was later demonstrated, and eliminated most of the observed jitter.

Blank areas in the upper portion of the vector plots are due to the presence of the time code and azimuth information inserted into the images. A notable feature in these vector plots was the counterclockwise roll up seen under the hub. This feature is most prominent in the 0 deg. and 330 deg. plots. The

remaining plots show a more upward trend in this area. The upward component on the right side of each plot may be indicative of the flow being pulled toward the tip vortex of the retreating blade. The results were poor in the lower left corner due to the presence of the tip vortex from the advancing blade. This was due to three problems. First, the spatial scales of the flow variations in the tip vortex are too small to be captured by the imaging system in its present form: the time delay between cameras is too long to obtain good correlation between successive sub-images, and the pixel resolution is too coarse to resolve the spatial scales. The resolution of the analysis was also not adequate to capture the large velocity gradients present in the tip vortex region. In this flow field, there are substantial out-of-plane velocities. The time between images was obviously short enough to maintain good correlation between images under these conditions, removing a major worry about the performance of the technique in such flows.

Rotor Wake Leading Edge

A second experiment was performed, visualizing a larger area in the wake of an isolated rotor. The area imaged was 46.46 x 34.48 cm. Fig. 5 shows two sets of results from the analysis. The main feature captured by SCV was the downstream convection of the rotor wake. Two distinct regions of tip vortices are seen in the flow visualization: these correspond to cross-sections of vortices from the two blades, 180 degrees apart in phase of origin. The rotation of the tip vortices was again not captured due to a lack of resolution. The upper right portions of the plots show an upward component which appears to correspond to the roll up under the hub seen in the previous experiment.

WHITE LIGHT, LARGE AREA EXPERIMENTS

Experimental Setup

An objective of intense interest in rotorcraft aerodynamic testing is the measurement of velocity and turbulence statistics over very large areas and volumes. For such applications, lasers are impractical for two reasons. First is the prohibitive cost and complexity of scaling up a laser to the power required to illuminate large areas. Second is the extreme difficulty in meeting safety requirements when operating high-power lasers in outdoor environments.

Some initial experiments with white light sheets over large areas proved encouraging enough to attempt measurement of the flow field in the area downstream of the rotor in the 16-foot Aeroelastic Rotor Test Facility at Georgia Tech. A Bell 222 tail rotor was operated in the facility at 300 RPM and 4-deg. collective pitch angle. The rotor shaft is oriented horizontally in the honeycomb-enclosed test section, with the wake exiting through an opening in the honeycomb at the end. The area downstream of the exit is 8.38 m long by 6.1 m wide. When the light sheets are placed at the centerline of the rotor, the distance to the lowest camera location, and the parameters of the video lenses dictate the largest field of view captured in each setting. Since this area was much smaller than the facility floor area, the measurement region was divided into sections each to be individually done. Symmetry was assumed about the centerline and half the room was divided into 15 sections, each 1.63 x 1.17 m. A schematic of the room layout and sectioning is shown in Fig. 6. A sketch of the general flow pattern in the room is shown in Fig. 7. A white light sheet was constructed from two 300 watt halogen lamps and cylindrical lenses. This produced a horizontal sheet that was placed 2.39 m above the floor. The flow was seeded with a theatrical fog generator. A single camera was utilized due to the lower velocities and the ability to capture them with the 60 Hz framing rate. The camera shutter was set at 1/1000 sec. The pixel to physical distance conversion was found by recording a grid board. The camera was placed at the center of a section pointing vertically and the flow recorded. This was repeated for each section.

Results

Due to the large areas, it was not possible to keep seeding in all areas. However, this is not a problem when the objective is to obtain turbulence statistics. Ensemble averaging of the vectors obtained at each location can be performed, if the technique is efficient enough to permit computation of a large number of velocity fields. A criterion is needed to determine whether adequate seeding is present in each sub-image before deciding whether to compute a velocity vector for that sub-image. For this, the average pixel intensity was computed, and sub-images with values below a chosen threshold were rejected. Note that there is no requirement for every pixel or even a majority of pixels to have an intensity above the background: a wisp of smoke captured in the sub-image is adequate to compute local velocity. For each section, twenty images were digitized and analyzed. The twenty were then ensemble averaged using the intensity criterion and average and root mean square values of each component of velocity were determined. The results for all sections were then assembled, producing the plots shown in Figs. 8-10. These plots are a top view of the horizontal plane 2.39 m above the floor. It is recognized that 20 samples are inadequate to obtain stable averages; however, for the present paper, demonstration of the procedure was deemed adequate. All computations were performed on a 33MHZ i486

computer. The average computation time per vector was under 0.9 seconds. The computed ensemble averages are indeed quite stable, and show the recirculating flow pattern with surprising clarity, despite the small number of samples used in averaging.

The gaps in the plots are due to an overestimation of the area covered by the camera. Due to distortion at the edges of the lens, vectors could not be accurately calculated on the outer edges of the digitized images. The average velocity plot (Fig. 8) shows the strong flow produced along the centerline of the facility by the rotor wake and the spreading of this wake as it approaches the far wall. The flow is slowed and turned and returns along the side wall. There also appears to be some recirculation and mixing between the wake and the return flow. This seems to be most evident in the corner. Figures 9 and 10 show the rms velocities along the centerline and perpendicular to the centerline, respectively. The rms values show the greatest fluctuations in the area of the wake and also tend to indicate the increased spreading and mixing of the wake. The large values of the fluctuations indicate the unsteadiness of the flow field.

DISCUSSION

These results demonstrate the applicability of SCV to both rotor flow fields and large area velocity characterization. The rotor experiments demonstrated the ability to measure velocity fields in a plane when large out of plane velocities exist. Here, the shutter exposure times and the time between images must be kept small in order to maintain good correlation. However, the technique works well with laser sheet thicknesses that are greater than those allowable in PIV techniques, so that substantial out-of-plane motion can be tolerated with minimal error. The technique is also rapid enough to permit computation of sufficient velocity fields to form azimuthal variation histories.

When these experiments were originally contemplated, it was believed that phase averaging of a large number of velocity vectors would be essential to get stable vector fields, since the cross-correlations were feared to be extremely noisy. The results are surprising in that no such averaging is needed: each vector field is quite stable. This fact reduces the amount of computation needed, and the wind tunnel run time, by two orders of magnitude. The entire flow visualization needed to get two components of velocity in the entire rotor wake came from a videotape lasting less than 15 minutes. This should be compared with the many months of run time taken to document the same two components in a similar rotor wake using phase-averaged laser Doppler velocimetry a few years ago. The resolution and stability of the computed vector fields can be greatly enhanced by iterative processing of the same set of flow images. This capability has been demonstrated and discussed in Refs. 2 and 3.

The white light sheet experiments demonstrated the ability to measure flow fields using longer shutter exposure times and less than ideal sheet characteristics. Note that continuous-wattage light sheets are used, with shutter exposures that are too long to ensure "freezing" of flow images. As a result, it is inevitable that some "streaking" of patterns must occur. During experiments performed by an undergraduate class in Winter '93, it was discovered that this streaking did not cause errors, since the streaks were captured identically on both cameras: thus the only effect of the streaking is to modify the patterns that are correlated. Following this discovery[5], it became possible to use such low-intensity sheets as that created from a 3-watt cw argon ion laser, even in the large rotor facility. This was then extended to the white-light experiments presented here. The light sheet thickness is on the order of 25 to 40mm, and there was a significant amount of background scattering from the bright white-painted walls and ceiling of the facility. The technique is still able to produce excellent results under such conditions.

Further development and refinement is still required. There are still limitations in measurement of the large velocity gradients present in the rotor flow field due to the tip vortices. An effort is underway to measure rotation of vortical structures directly from flow images. Additional improvements in experimental equipment and technique are currently being developed. The ability to synchronize the camera shutters and the laser pulses to more accurately determine time delays between images is being implemented. Resolution in the rotor flow field can also be improved by increasing the number of cameras.

In the large area case, velocity gradients are usually mild and can easily be captured with current SCV methods. In this case, the difficulties are mainly with automating the set-up and in devising means of efficiently seeding large areas. Controlling the divergence of the beams would permit more efficient use of the available light. However, the surprising ability to use moderately long shutter exposure times removed a major constraint, and enables the use of inexpensive continuous-wattage sources.

CONCLUSIONS

1. Instantaneous planar velocity fields have been successfully measured in rotor wakes in hover and forward flight.

2. The SCV technique has been demonstrated successfully in flows with strong out-of-plane velocity components.
3. Roll-up of the wake under the hub of a 2-blade rotor in forward flight has been quantitatively captured.
4. Stable and consistent velocity fields are obtained without ensemble-averaging in a rotor wake.
5. Improvements for resolving velocity in regions of high shear are still needed.
6. Velocity statistics can be determined piecewise over very large areas using the SCV technique.
7. Inexpensive white light sources can be used in the SCV technique, with a fully numerical post-processing algorithm.
8. Computation times of less than one second per vector have been demonstrated using a 33MHz i486 personal computer.
9. The SCV technique can be used effectively on images where the shutter exposure time is too long to freeze the motion of the particles.
10. Due to the ability to use moderately long exposure times, SCV works with continuous-wattage sources.
11. Ensemble averaging using an intensity criterion is an effective method to determine velocity statistics in areas with inconsistent seeding.
12. The flow in the settling area of a large rotor hover test facility is characterized by a strong, central wake that spreads and slows before turning at the back wall. Most of the facility has very slow, recirculating flow.

REFERENCES

1. Komerath, N.M., Fawcett, P.A., "Planar Velocimetry by Spatial Cross-Correlation: Theoretical Basis and Validation". AIAA 90-1634, Fluid Dynamics Conference, June 1990.
2. Fawcett, P.A., Komerath, N.M., "Spatial Correlation Velocimetry in Unsteady Flows." AIAA 91-0271, 22nd Aerospace Sciences Meeting, Reno, NV, January 1991.
3. Fawcett, P.A., Funk, R.B., Komerath, N.M., "Quantification of Canard and Wing Interactions Using Spatial Correlation Velocimetry." AIAA 92-2687, 10th Applied Aerodynamics Conference, June 1992.
4. Fawcett, P.A, An Investigation on Planar Velocimetry by Spatial Cross Correlation. Ph.D. Thesis, School of Aerospace Engineering, Georgia Institute of Technology, September 1992.
5. Lynn, J., and Hamel, T., Laboratory Report, AE4010, Winter '93, School of Aerospace Engineering, Georgia Institute of Technology. Guided by Dr. N.M. Komerath

ACKNOWLEDGMENTS

This work was supported by the U.S. Army Research Office under Rotorcraft Center Contracts No. DAAL03-88-C-0003-AD2, Aerodynamics Task 2 and DAAH-04-93-G-0002-AD3, Aerodynamics Task 3. Dr. T. L. Doligalski is the Technical Monitor. The first author is partially supported by a National Science Foundation Graduate Fellowship. CM-2 usage was supplied under Grant CBT900058P from the Pittsburgh Supercomputing Center.

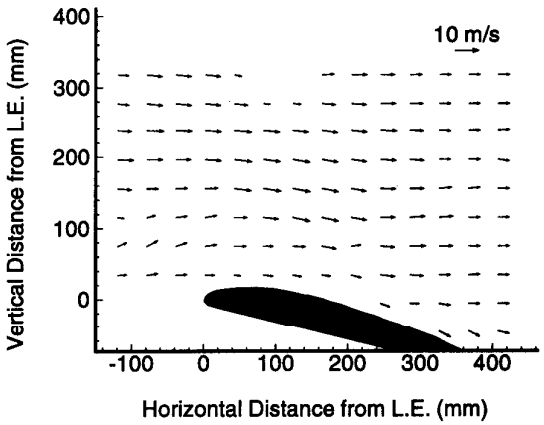

Figure 1: Sample Canard/Wing Vector Plot

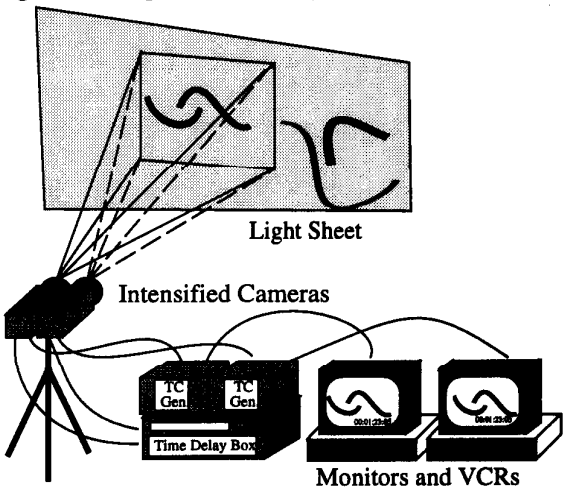

Figure 2: Experimental Imaging Setup

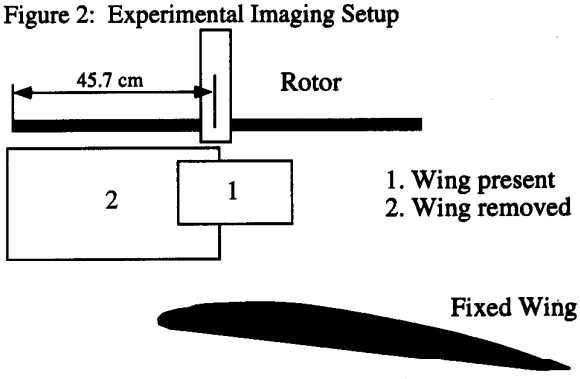

Figure 3: Rotor Setup with Image Sections

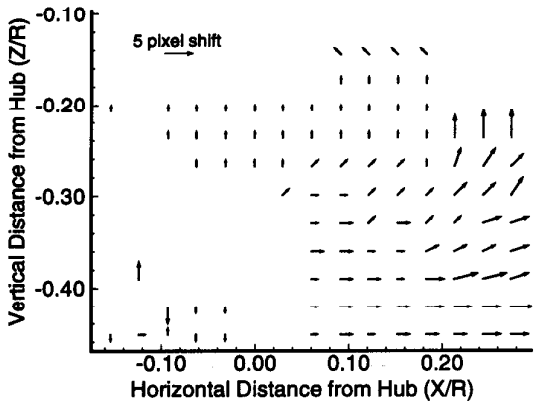

a) $\Psi = 0$ degrees

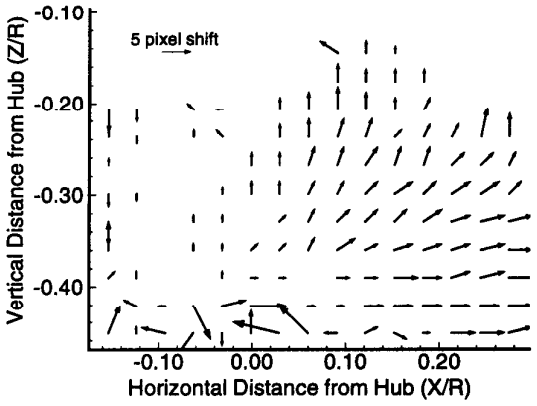

d) $\Psi = 90$ degrees

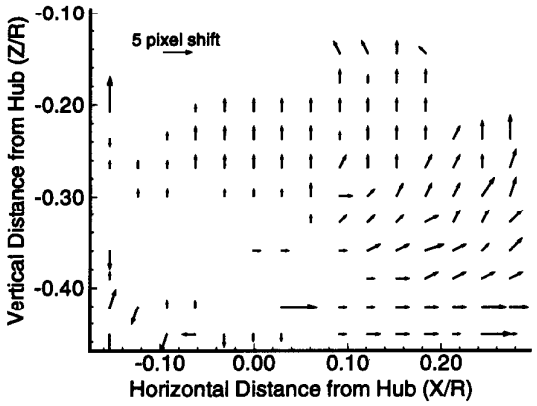

b) $\Psi = 30$ degrees

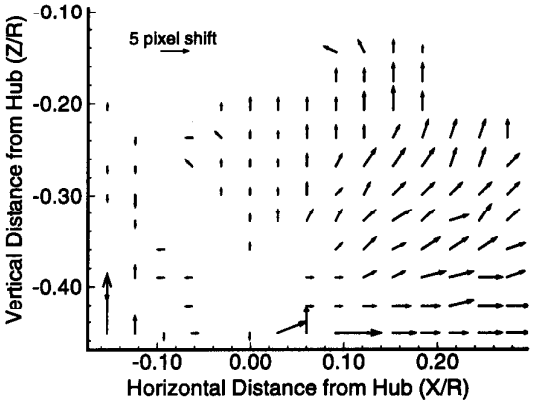

e) $\Psi = 120$ degrees

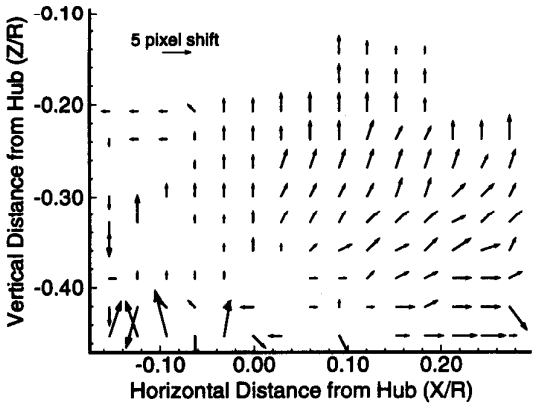

c) $\Psi = 60$ degrees

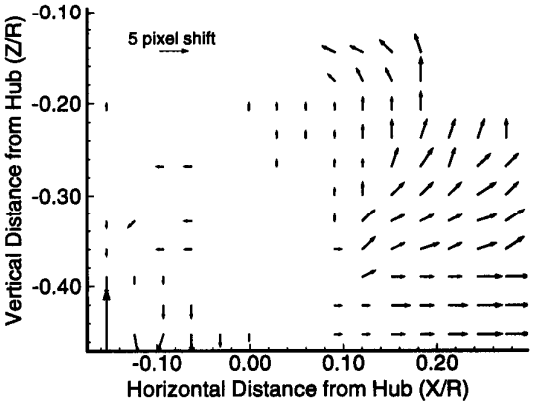

f) $\Psi = 150$ degrees

Figure 4: Rotor/Wing Vector Plots, $\mu = 0.075$

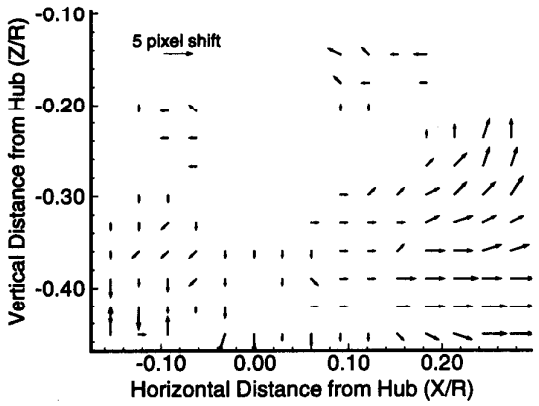

g) $\Psi = 180$ degrees

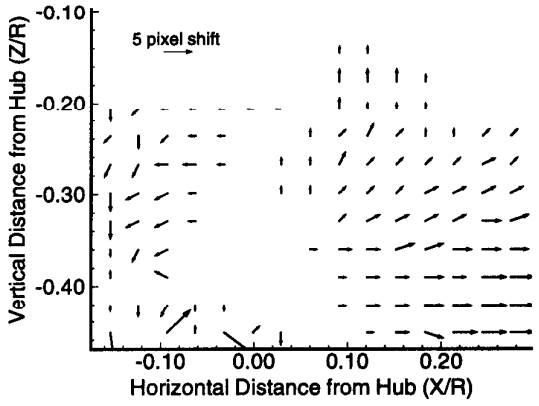

j) $\Psi = 270$ degrees

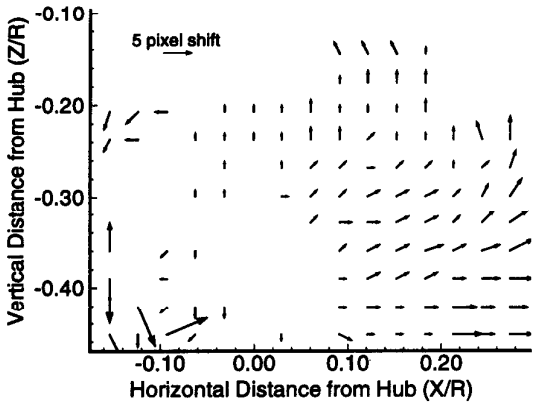

h) $\Psi = 210$ degrees

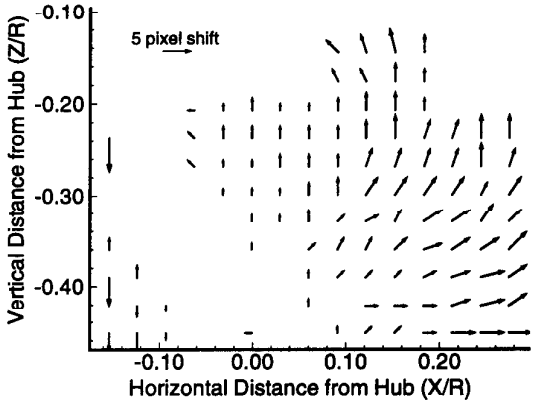

k) $\Psi = 300$ degrees

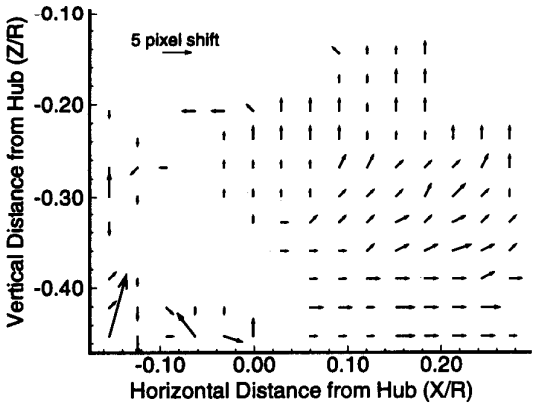

i) $\Psi = 240$ degrees

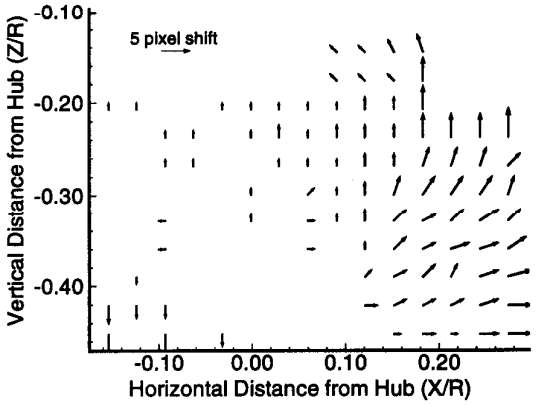

l) $\Psi = 330$ degrees

Figure 4 (cont): Rotor Wing Vector Plots, $\mu = 0.075$

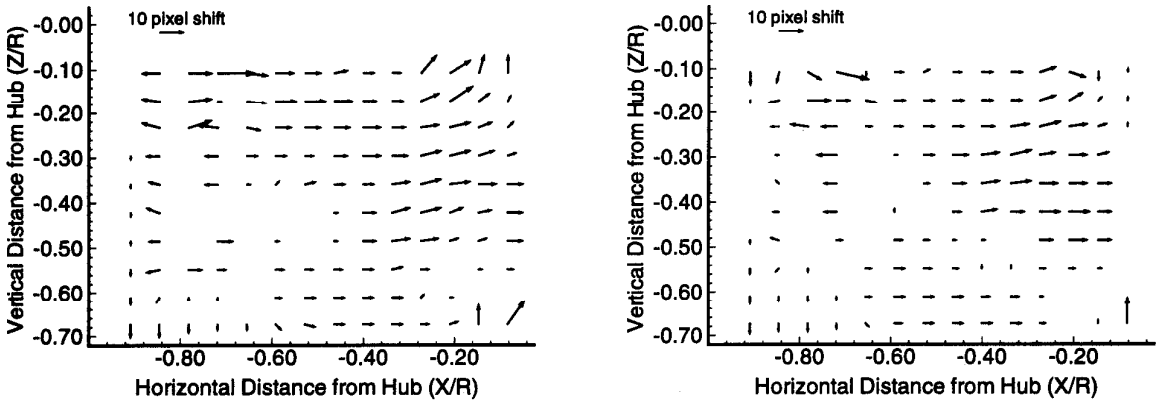

a) $\Psi = 175$ degrees

b) $\Psi = 315$ degrees

Figure 5: Isolated Rotor Vector Plots, $\mu = 0.075$

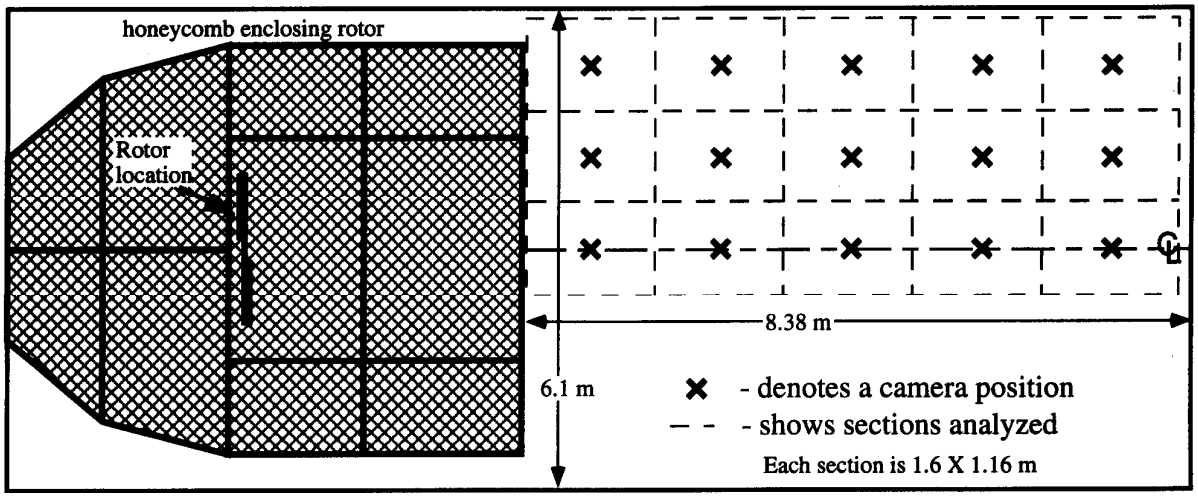

Figure 6: Schematic of Aeroelastic Test Facility and Camera locations

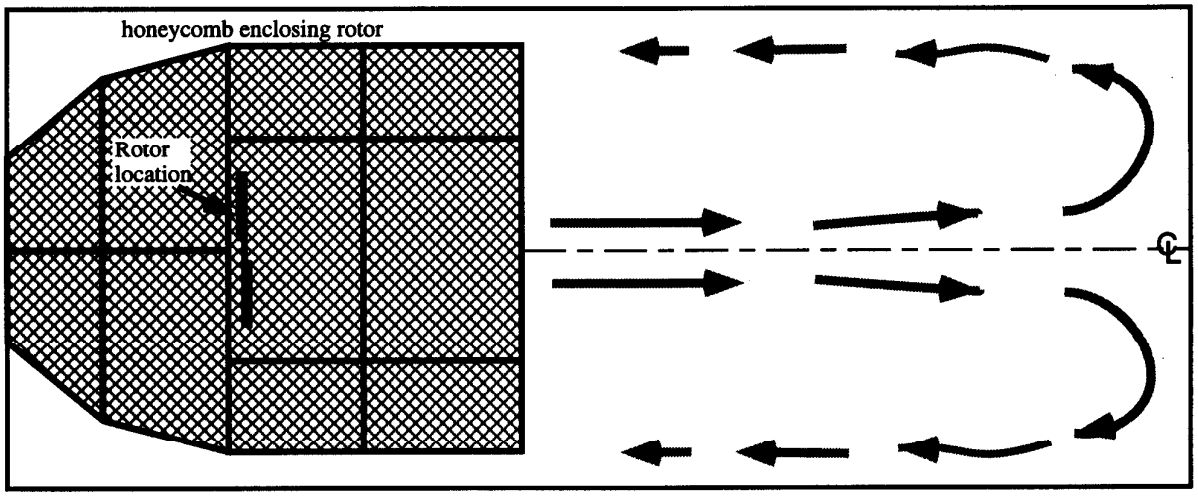

Figure 7: General Flow Field in the Aeroelastic Test Facility

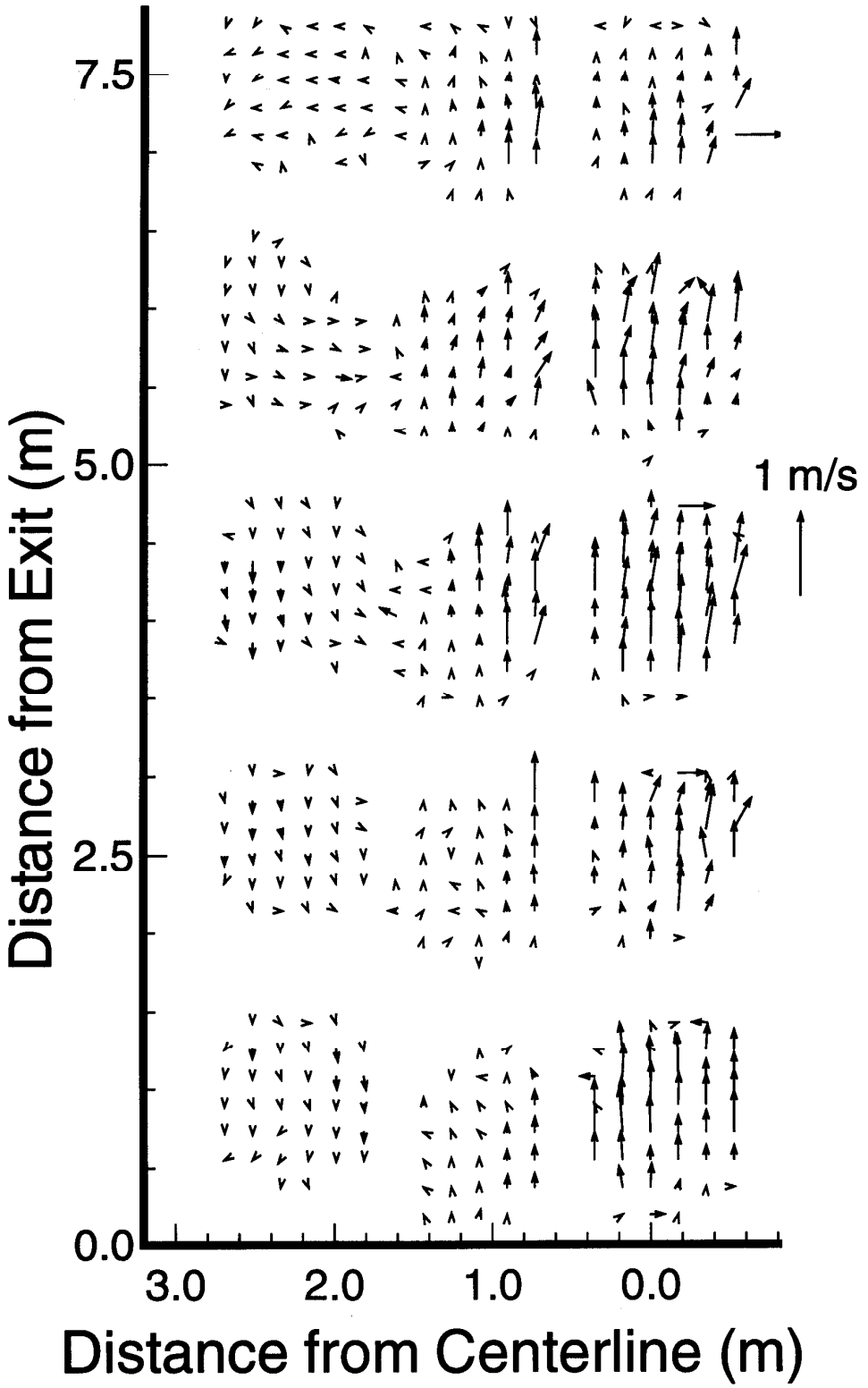

Figure 8: Averaged Velocities in the Test Facility

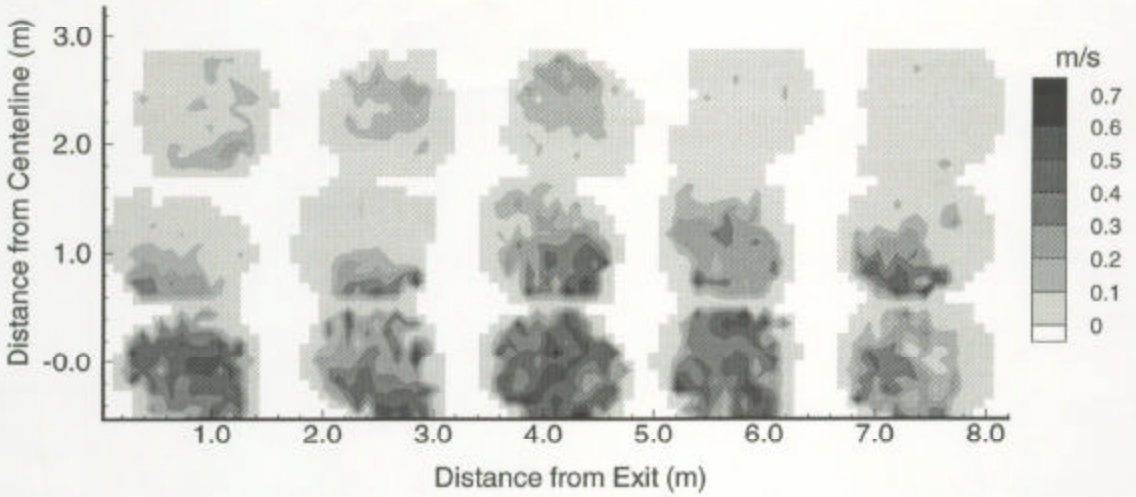

Figure 9: Contour Plot of the RMS fluctuations in velocity component parallel to the centerline in the rotor test facility

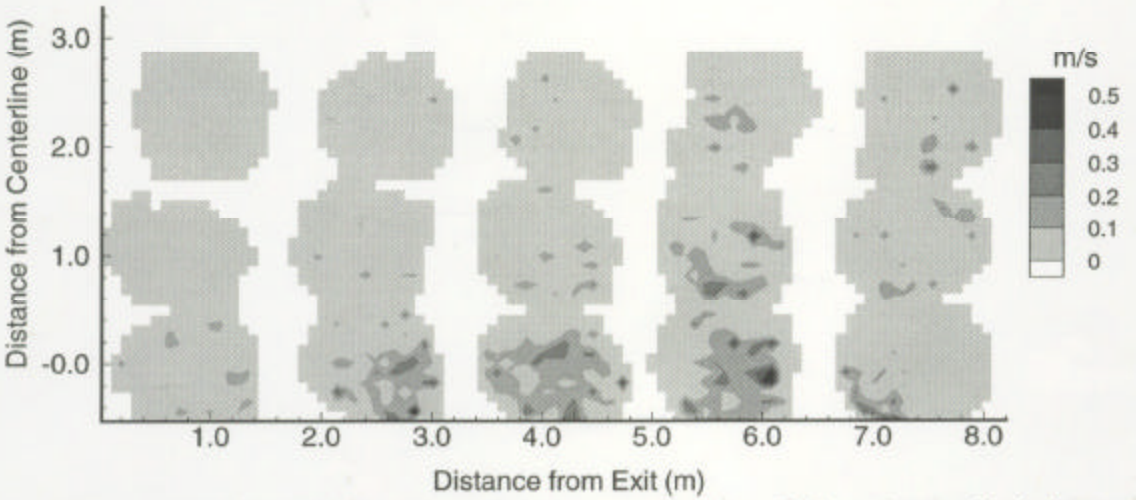

Figure 10: Contour Plot of the RMS fluctuations in velocity component perpendicular to the centerline in the rotor test facility